Cerebral Cortex November 2013;23:2620–2631
doi:10.1093/cercor/bhs241
Advance Access publication August 28, 2012

Coupling Diffusion Imaging with Histological and Gene Expression Analysis to Examine the Dynamics of Cortical Areas across the Fetal Period of Human Brain Development

Hao Huang[1,2,3], Tina Jeon[1], Goran Sedmak[4,5], Mihovil Pletikos[4,5], Lana Vasung[5], Xuming Xu[4], Paul Yarowsky[6], Linda J. Richards[7], Ivica Kostović[5], Nenad Šestan[4] and Susumu Mori[3]

[1]Advanced Imaging Research Center [2]Department of Radiology, University of Texas Southwestern Medical Center, Dallas, TX 75390, USA [3]Department of Radiology, Johns Hopkins University School of Medicine, Baltimore, MD 21205, USA [4]Department of Neurobiology and Kavli Institute for Neuroscience, Yale University, New Haven, CT 06510, USA [5]Croatian Institute for Brain Research, University of Zagreb, Zagreb, Croatia [6]Department of Pharmacology and Experimental Therapeutics, University of Maryland School of Medicine, Baltimore, MD 21201, USA [7]The Queensland Brain Institute and the School of Biomedical Sciences, University of Queensland, St Lucia 4072, Australia

Address correspondence to Hao Huang, Advanced Imaging Research Center, University of Texas Southwestern Medical Center, 5323 Harry Hines Blvd, Dallas, TX 75390-8542, USA. Email: hao.huang@utsouthwestern.edu

As a prominent component of the human fetal brain, the structure of the cerebral wall is characterized by its laminar organization which includes the radial glial scaffold during fetal development. Diffusion tensor imaging (DTI) is useful to quantitatively delineate the microstructure of the developing brain and to clearly identify transient fetal layers in the cerebral wall. In our study, the spatio-temporal microstructural changes in the developing human fetal cerebral wall were quantitatively characterized with high-resolution DTI data of postmortem fetal brains from 13 to 21 gestational weeks. Eleven regions of interest for each layer in the entire cerebral wall were included. Distinctive time courses of microstructural changes were revealed for 11 regions of the neocortical plate. A histological analysis was also integrated to elucidate the relationship between DTI fractional anisotropy (FA) and histology. High FA values correlated with organized radial architecture in histological image. Expression levels of 17565 genes were quantified for each of 11 regions of human fetal neocortex from 13 to 21 gestational weeks to identify transcripts showing significant correlation with FA change. These correlations suggest that the heterogeneous and regionally specific microstructural changes of the human neocortex are related to different gene expression patterns.

Keywords: development, diffusion tensor imaging, gene expression, histology, human fetal brain

Introduction

Human fetal brain development is an immensely complicated process. As a prominent component of the fetal brain, the cerebral wall (pallium) is the place where extremely complicated yet highly organized developmental processes occur during fetal development to form the adult cerebral cortex. These developmental processes include proliferation, cell differentiation, synapse formation, axonal and dendritic growth, molecular specification, neural aggregation, and myelination. The fetal cerebral wall is characterized by a laminar organization (Kostović et al. 2002; Kostović and Vasung 2009) with some transient layers lacking their direct counterparts in the adult brain. From this initial phase of expansion and differentiation, the anatomical (e.g. Toga et al. 2006) and cytoarchitectonic organization (e.g. Economo and Koskinas 1925) of the adult cerebrum emerges. Unique spatio-temporal signatures of the developmental processes in different regions of the cortical plate and subplate (Kostović and Rakic 1990; Rakic et al. 1991; Vasung et al. 2010), the 2 outmost layers of the cerebral wall, are visible with magnetic resonance imaging (MRI), and underlie the regional formation of distinct areas.

Knowledge regarding the dynamic events occurring during the development of the fetal cerebral cortical structures has been largely based on previous histological findings in primates and rodents (e.g. Rakic 1972, 1988; Caviness 1982; Levitt et al. 1997; Del Rio et al. 2000; Bystron et al. 2008). The seminal discoveries of neuronal migration along radial glial fibers (Rakic 1972, 1995; Sidman and Rakic 1973) and the subplate zone (Kostović and Molliver 1974; Kostović and Rakic 1980, 1990; Allendoerfer and Shatz, 1994) have provided an important fundamental understanding of the architecture of the fetal cerebral wall. Cortical neurons are generated in the ventricular and subventricular zone and migrate toward the cortical plate along the radial glial scaffold. In the cortical plate, migrating neurons interact with each other or with existent neurons of the cortical plate through synaptic formation, dendritic, and axonal growth (Sidman and Rakic, 1973; Kwan et al. 2012). The subplate is a transient layer located just beneath the cortical plate and plays a key role in neurodevelopment as afferents from the thalamus temporarily reside in the subplate, establish synapses, and take part in cellular interactions that are crucial for subsequent cortical development.

Based on previous findings with histological imaging, which remain an outstanding tool to study the cerebral wall of developing human brains (Sidman and Rakic 1982; Honig et al. 1996; Bayer and Altman 2004, 2005; O'rahilly and Műller 2006), 3D MRI could bring us further insights into the complicated spatio-temporal processes that occur during the development of human cerebral cortex. Diffusion tensor imaging (DTI) (Moseley et al. 1990; Basser et al. 1994), one type of MRI, is especially useful to delineate the anatomy of the developing human and animal brain (Hüppi et al. 1998; Neil et al. 1998; McKinstry et al. 2002; Mukherjee et al. 2002; Neil et al. 2002; Maas et al. 2004; Partridge et al. 2004; deIpolyi et al. 2005; Huang et al. 2006, 2009; Takahashi et al. 2012; Thornton et al. 1997; Mori et al. 2001; Zhang et al. 2003, 2005; Kroenke et al. 2007; Sizonenko et al. 2007; Huang et al. 2008; Kroenke et al. 2009; Takahashi et al. 2011). DTI is sensitive to anisotropic diffusion of water molecules along ordered structures such as axon tracts and radial glia. Fractional anisotropy (FA), derived from diffusion tensor and ranging from zero to one, quantifies the extent of the aligned

structures. In the fetal stage, FA values of the cortical plate are high (Thornton et al. 1997; Neil et al. 1998; Mori et al. 2001; McKinstry et al. 2002) because of the dominant organized columnar structures in the cortex. The disruption of the columnar structures due to loss of radial glia, synapse formation, and increased dendritic density (McKinstry et al. 2002; Huang et al. 2008) results in a decrease in FA values. Hence quantifying this pattern of decrease in the FA can be used to correlate at a regional level, neural processes such as synaptic formation, axonal and dendritic growth in the cortical plate, and to investigate region-specific maturation and differentiation. The unique patterns of decrease in FA values in different cortical regions have been examined in rodents (Huang et al. 2008). However, there have been few studies mapping the FA over the entire cerebral wall and characterizing the time course of FA values for local cortical regions of human fetal brains.

While high-resolution DTI can provide detailed and quantitative information regarding the microstructural changes of the cortical plate and cerebral wall, the mechanisms underlying these microstructural changes remain elusive. The development of the human brain depends on the diversity and precise spatio-temporal regulation of its transcriptome. Variations in the transcriptional regulation of key developmentally expressed genes are thought to have led to the creation of new combinatorial expression patterns from a relatively limited set of genes, and ultimately to the formation of distinct cortical regions. With transcriptome analysis, regional differences in gene expression in the developmental cortical plate has been delineated (Johnson et al. 2009; Kang et al. 2011). This type of study provides unique information regarding gene expression and can be utilized to form a cortical map of gene profiling (Hawrylycz et al. 2010). Correlating the microstructural data from DTI and gene expression data can reveal the molecular and cellular processes underlying the structural changes observed with DTI.

In this study, we combined DTI, gene analysis, and histology to qualitatively and quantitatively delineate regional microstructural changes of all layers in the cerebral wall. The goal was to provide a comprehensive and detailed quantitative characterization of the complicated spatio-temporal microstructural development of the cerebral wall and to ultimately elucidate the relationship between the microstructural changes observed by DTI and gene expression. High-resolution and high signal-to-noise ratio (SNR) DTI data and histology of postmortem human fetal brain tissue from 13 to 21 weeks of gestation (wg; corresponding approximately to 11-19 weeks post-conception) were acquired. Eleven cortical regions, encompassing some major anatomical areas of the neocortex, were manually delineated. With three clearly identified layers from the FA map, namely the cortical plate, subplate, and an inner layer (including the intermediate zone, the subventricular zone, the periventricular zone, and the ventricular zone), the FA values at all cortical regions in all 3 layers were measured. A time course of FA values for each cortical region was characterized and compared. This allowed us to divide the developmental process into 2 stages, 13–15 and 17–21 wg, since we detected significant changes of FA from early to mid-fetal developmental period (Kostović and Vasung 2009) in all brain regions. The FA distribution overall was heterogeneous across the cerebral wall and distinct temporal changes of cortical FA values were observed across different regions. In parallel, 17565 genes were quantified in these same 11 brain regions from 9 brains in the same period. A correlation analysis was conducted to identify the genes that significantly correlated with a microstructural metric characterizing FA changes during late mid-fetal developmental period.

Materials and Methods

Fetal Brain Samples

Fetal brain samples were obtained from the University of Maryland Brain and Tissue Bank for Developmental Disorders (NICHD Contract No. N01-HD-4-3368 and N01-HD-4-3383). The samples were fixed with 4% paraformaldehyde (PFA) in phosphate-buffered saline (PBS) and later used for both DT-MRI and histology. Three to 6 fixed postmortem fetal brains at each gestational week between 13 and 21 wg were scanned to acquire high-resolution DTI data. Owing to extreme fragility of the tissue, some tissue was unfortunately damaged in transit or during the experiment resulting in only 2–3 datasets at each time point being able to be included in this study. Specifically, DTI datasets from two 13 wg, two 15 wg, two 17 wg, three 19 wg, and two 21 wg fetal brains, covering both early and mid-fetal developmental period, were used in this study. Additionally, gene expression analysis was done from brains with corresponding ages using data from NCBI Gene Expression Omnibus under accession number GSE25219, as previously reported by Kang et al. 2011.

DTI Data Acquisition

Fetal brain samples between 13 and 21 wg were kept immersed in the fixation solution until 48 h before the MR experiments. The samples were then transferred to PBS to wash out the fixative. The samples were then immersed in PBS in a custom-made MR compatible chamber throughout the MR scanning. 3D multiple spin echo DTI was performed in both 11.7-T and 4.7-T Bruker scanners. A multiple echo (number of echoes = 8) sequence was adopted to improve the SNR. Thirteen to 16 week fetal brains were scanned in an 11.7-T Bruker scanner with a micro 2.5 30-mm inner diameter Bruker volume coil. Fetal brains over 17 weeks gestation were scanned in a 4.7-T Bruker scanner with a 70-mm inner diameter Bruker volume coil. These volume coils were used as the radio frequency signal transmitter and receiver. A set of diffusion-weighted images (DWIs) were acquired in 7 linearly independent directions. Diffusion-sensitizing gradients with a b value of 1000 s/mm^2 were applied along 6 different orientations: [0.707, 0.707, 0], [0.707, 0, 0.707], [0, 0.707, 0.707], [−0.707, 0.707, 0], [0.707, 0, −0.707], [0, −0.707, 0.707]. DWI parameters for the 11.7-T scanner were effective TE (time to echo) = 67 ms, TR (repetition time) = 0.8 s, FOV (field of view) = 25–35/25–35/25–35 mm, and imaging matrix = 128 × 80 × 80 (zero filled to data matrix = 128 × 128 × 128). The imaging resolution was 200–400 µm for fetal brains between 13 and 16 weeks of gestation. DWI parameters for the 4.7-T scanner were effective TE = 66 ms, TR = 0.8s, FOV = 40–52 mm/40–52 mm/40–52 mm, and imaging matrix = 128 × 72 × 72 (zero filled to data matrix = 128 × 128 × 128). The imaging resolution was 300–600 µm for fetal brains between 17 and 21 weeks of gestation. The total imaging time was approximately 20 h per brain with 2 signal averages for DTI data acquisition at both 4.7 and 11.7 T.

Histology and Histology-DTI Correlation

Histology

After DTI data acquisition, some of the fixed postmortem brain tissues were sectioned for histological analysis. These samples were immersed in 10–30% sucrose in 4% PFA for 2–3 days until they sank in the solution, then frozen in liquid 2-methylbutane at −20°C. Frozen brains were serially sectioned at 80 µm on a freezing microtome. Sections were stored in a cryoprotectant solution and then transferred

into PBS just prior to immunohistochemistry. The immunohistochemistry was performed on floating sections. Sections of postmortem brains were rinsed in PBS before they were blocked in 2% normal goat serum. After they were stained with hematoxylin, or immunohistochemically labeled with anti-glial fibrillary acidic protein (GFAP) antibody and neurofilament (NF) antibody, the sections were mounted onto gelatinized glass slides, dehydrated through increasing concentrations of ethanol, immersed in 2 changes of Histo-Clear solution, and coverslipped with DPX mounting medium.

Histology-DTI Correlation

All DTI data were acquired with a 3D sequence and had almost cubic resolution. For a selected histological image, the 3D DTI data of the same age were rotated and a corresponding coronal or axial slice of DTI image was chosen to match the histological section. FA quantification of the small segments of cerebral wall corresponding to those from GFAP and NF histological images was based on a manual selection of regions of interest (ROIs). We further segmented 3 layers, namely layer 1, layer 2, and layer 3 from cortical plate to ventricle, with the contrasts observed from hemotoxylin-stained sections of a 15-wg brain. The segmented regions derived from the hematoxylin-stained sections were used directly as ROIs to measure the FA values on the corresponding FA map. This process required registering the 2 images in a manner that allowed for fine-tuning the FA map to match its corresponding histological image. The registration was conducted with large deformation diffeomorphic metric mapping (LDDMM, Miller et al. 2002). The outermost layer (layer 1) segmented from hematoxylin-stained contrast is the cortical plate. The other 2 layers, layer 2 and layer 3, of the hematoxylin-stained histological image matched the subplate and the inner layer observed by the contrast of the FA maps, respectively. When calculating the FA in each layer defined by the hematoxylin-stained histological image, we applied a threshold of 0.1 for layer 1 and layer 3 to remove any residual mismatched voxels from the ROI.

FA measurement of the Cerebral Wall

Cortical Mapping of the FA

The FA values on the cortical surface were projected from the cortical plate, the outermost layer of the cerebral wall. The entire brain was segmented using the intensity thresholding of the averaged diffusion weighted images (aDWIs). Triangular meshes were then created by using Amira software (Mercury) from the isosurface function, which defined the cortical surface. On each triangular vertex, an FA value was assigned by reading the FA value of the pixel closest to the inside of the brain. For the triangular vertex which does not completely intersect the cortical plate, a cubic box with 5 voxels on each side and centered at the vertex was established and the maximum FA value of this cubic box ROI was assigned as the FA value of this triangular vertex.

Manual Delineation of Surface ROIs

To obtain the surface ROIs, surface editing functions in Amira software were used to directly delineate these ROIs from the 3D reconstructed cortical surface. Eleven ROIs were manually placed on the cortical surface of all fetal brains examined, following previously published descriptions (Johnson et al. 2009; Kang et al. 2011). These ROIs represented the orbital prefrontal cortex (OFC), dorsolateral prefrontal cortex (DFC), medial prefrontal cortex (MFC), ventrolateral prefrontal cortex (VFC), motor cortex (M1C), somatosensory cortex (S1C), posterior inferior parietal cortex (IPC), primary auditory cortex (A1C), posterior superior temporal cortex (STC), inferior temporal cortex (ITC), and primary visual (occipital) cortex (V1C). The corresponding ROIs from DTI and gene profiling are shown in Figure 1. These ROIs served as the bridge between the DTI and gene expression data, underlying the correspondence of datasets from the 2 categories. The manual delineation of the ROIs from the reconstructed cortical surface using DTI data was performed by trained neuroanatomists (G.S. and M.P.), who identified, dissected and defined the ROIs with the same neuroanatomical criteria to that used for the dissection of the tissue for gene expression analysis (Johnson et al. 2009; Kang et al. 2011).

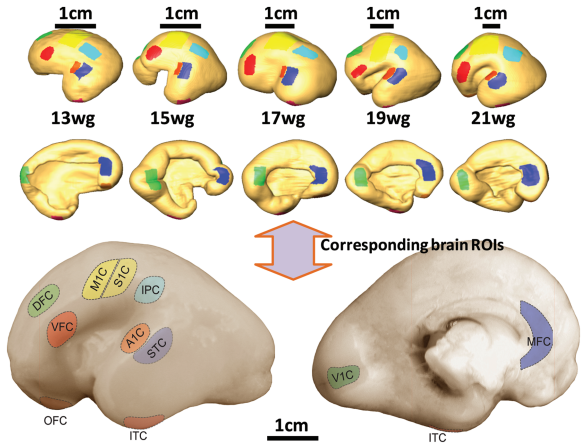

Figure 1. Upper images represent the cortical surface reconstructed from DTI data and the lower images demonstrate the location of the tissues for transcriptome analysis. The corresponding 11 cortical ROIs (DFC, VFC, MFC, OFC, M1C, S1C, IPC, A1C, STC, ITC, and V1C) for both types of data are shown with the same color. In the upper panel, upper and lower rows demonstrate the lateral and medial views of the cortical surfaces, respectively. DFC, dorsolateral prefrontal cortex (PFC); VFC, ventrolateral PFC; MFC, medial PFC; OFC, orbital PFC; M1C, motor cortex; S1C, somatosensory cortex; IPC, posterior inferior parietal cortex; A1C, primary auditory cortex; STC, posterior superior temporal cortex; ITC, inferior temporal cortex; V1C, primary visual (occipital) cortex.

Segmentation of the Cerebral Wall into 3 Layers

The parcellation of the 3 layers in the cerebral wall was conducted manually using ROIEditor (www.mristudio.org). The manual parcellation of each cerebral layer was conducted 3 times. Dice ratios (Dice 1945) between any 2 segmentations of the same layer were above 95%, indicating good reproducibility.

Regional FA Measurements of Each Cortical Region and Layer

After the surface meshes of each of the 11 cortical surface ROIs were projected perpendicularly into the 3 layers, 3 volume format binary masks were generated serving as the volumetric ROI in each of 3 cerebral layers and corresponding to cortical surface ROI. In total, 33 volumetric ROIs covering all 3 layers were obtained. The mean, standard deviation, maximum, third quartile, median, first quartile, and the minimum values of the FA were measured with these volumetric format ROIs.

Statistical Comparison of the FA's Between the Early and Mid-Fetal period for All Volumetric Format ROIs

To ensure an equal weighting of FA measurements were obtained from each dataset, the same amount of values were sampled from FA measurements of each volumetric ROI in one of the 3 layers. FA measurements for each layer were separated into 2 groups based on the gestational stage. FA values of 13–15 wg formed 1 group and those of the 17–21 wg formed another group. The FA values of the 2 groups were compared with a Student's *t*-test. Bonferroni's correction (Bonferroni 1936; Shaffer 1995) was applied to avoid the spurious positives when rejecting the null hypothesis. Instead of using a threshold of 0.05 for *P* values, 0.05/11 or 0.0045 was used to lower the threshold and account for the number of comparisons being performed.

Inter-Region Comparison of Time Courses of Cortical Plate FA

The FA values of 11 regions of the cortical plate were plotted with the gestational age as a variable to reveal a time course of regional cortical FA which showed a significant decrease during fetal development.

Moreover, the heterogeneity of the regional FA decrease in the cortical plate was tested with a Mann–Whitney statistics. Similar to the statistical model we previously used (Huang et al. 2008), it was defined as

$$M = \sum_{t=1}^{T} \sum_{k=1}^{N} (Rk(1,k,t) + Rk(2,k,t) - 2N - 1)^2 , \quad (1)$$

where i, k, and t indicated considered specimen, region, and time point, respectively and $Rk(i,k,t)$ was the rank of FA(i,k,t) in the sequence of $2N$ numbers FA(1,1,t), FA(2,1,t), … , FA(1,N,t), FA(2,N,t), for fixed time t. t was from 1 to T (T = 5) and k was from 1 to N (N = 2). In this model, each group had 2 specimens and this has been hard coded in equation (1). For the 19 wg brains, 2 of 3 specimens were randomly chosen for analysis. Note that N was always 2 as statistical comparisons were conducted with 2 groups. We then calculated the M_{MC} value of each randomly generated sequence, where MC indicated Monte Carlo samples. Because, under the null hypothesis, all sequences of the ranks have the same probability, a P value for the observed M (calculated from our data with equation [1]) could be computed as the proportion of Monte Carlo samples that were above it. More precisely, if there were N_{MC} Monte Carlo simulations and N_{lessM} was the number of simulations in which M_{MC} values were less than the observed M, we computed the P values from M as follows, $P = 1-(N_{lessM}+0.5)/N_{MC}$. For multiple-comparison correction, Bonferroni's correction (Bonferroni 1936; Shaffer 1995) was also used with a smaller P value 0.05/11 as a threshold of significant difference.

Correlation of Gene and Microstructural Measures

Quantification of Cortical FA Changes from Early to the Mid-Fetal Developmental Period

At the cortical locations $\boldsymbol{x}$ which correspond anatomically to those used for gene expression analysis, FA values at each time point t, that is, 13, 15, 17, 19 and 21 wg, were measured. For each time point, we obtained usable DTI data from 2 or 3 brains, represented by $k(t)$. FA ($\boldsymbol{x}$, $k(t)$,t) then indicated the FA measurement at a cortical area and a certain time point of a specific fetal brain. The FA ratio of a cortical area $\boldsymbol{x}$ was defined as the average of FA measurements of all fetal brains in the early fetal period divided by the average FA measurements of all fetal brains in mid-fetal period:

$$\text{ratio}(x) = \frac{\sum_{t=13-15\,\text{wg}} \sum_k \text{FA}(\boldsymbol{x}, k(t), t) / \sum_{t=13-15\text{wg}} k(t)}{\sum_{t=17-21\text{wg}} \sum_k \text{FA}(\boldsymbol{x}, k(t), t) / \sum_{t=17-21\text{wg}} k(t)}$$

From this equation, it can be appreciated that the defined FA ratio is a function of the cortical area $\boldsymbol{x}$ only and reflects the level of the FA decrease from early to mid-fetal developmental period.

Gene Analysis

The gene analysis was done using data from NCBI Gene Expression Omnibus under accession number GSE25219 (Kang et al. 2011), with matched ages. The method for gene analysis was previously described (Johnson et al. 2009; Kang et al. 2011).

Identification of Gene Expression Correlated with FA Changes during Fetal Development

A total of 17565 genes were quantified for each of 11 cortical ROIs from each specimen used for gene analysis (see Kang et al. 2011 for details). Then for each gene, a vector consisting of the average expression levels in the 11 neocortex ROIs was constructed. In parallel, spatio-temporal FA measurements were obtained. Using the metric of the FA ratio, the temporal change of FA at each region was simplified into a scalar value. The FA ratio vector was composed of FA ratios from all cortical ROIs. Without a priori knowledge, a correlation coefficient and a nominal P value from the Pearson correlation between each scalar vector of expression of N (N = 17565) genes and the FA ratio vector were calculated. All nominal P values for 17565 genes were adjusted using a Benjamini–Hochberg false discovery rate (FDR) approach. The top 5 and top 10 genes whose scalar vectors of expression were most significantly correlated to FA ratio vector were plotted and tabulated,(Fig 9, Table 2) respectively.

Results

Three Layers in the Cerebral Wall Delineated by DTI

As shown in the FA map in Figure 2, 3 layers can be clearly differentiated in most regions of the cerebral wall, except those undergoing cortical folding. They are the cortical plate (with marginal zone), subplate, and an inner later. It is noted that the inner layer can be further differentiated into multiple zones, namely the intermediate zone (fetal white matter), the subventricular cellular zone, the periventricular fiber-rich zone, and the ventricular zone, with histology (Kostović et al. 2002). As these zones within the inner layer cannot be delineated with FA map, we have integrated them as 1 for FA measurements. The term "inner layer" is solely for simplification as it is anatomically located at the most inner part of the cerebral wall, next to the ventricle.

A DTI Database of Developing Fetal Brain and Cortical Mapping of FA Values

A fetal brain DTI database that delineated the detailed anatomy of neural structures of fetal gray and white matter was established using high-resolution and high-contrast images including a DTI color-encoded map and an FA map, as shown in Figure 3. The laminated cerebral wall, which is the focus of this study, is the major structure of the developing human fetal brains at the ages examined. The 3 layers of the cerebral wall described above could be differentiated at each of time points from the FA maps (Fig. 3). The cerebral wall was traced with yellow curves and the layers inside were delineated by red curves. Qualitative and general trends of the

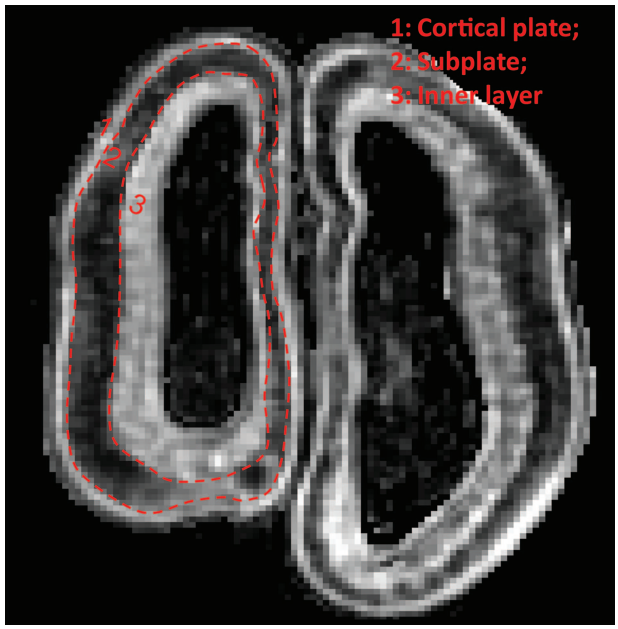

Figure 2. Three layers from the pial surface to the ventricle are the cortical plate (designated layer 1), subplate (designated layer 2), and the inner layer (designated layer 3), and can be clearly identified with the FA map of a typical second trimester fetal brain at 17 wg.

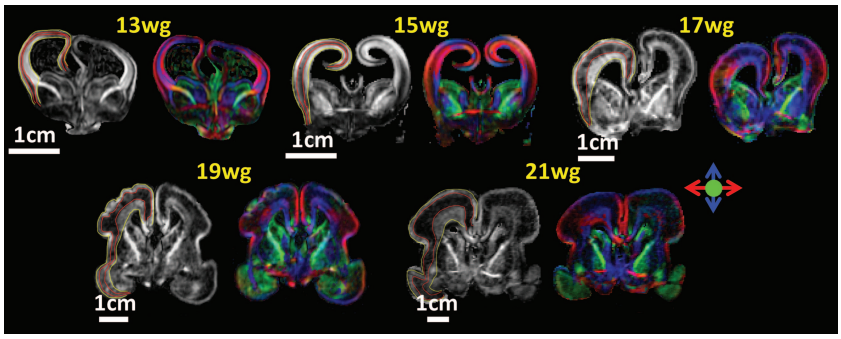

Figure 3. Coronal images of FA (left in each pair) and color-encoded FA map (right in each pair), both derived from DTI, of 13, 15, 17, 19, and 21 wg fetal brains are shown. Red, blue, and green in color-encoded FA map encodes left-right, superior-inferior, and anterior-posterior orientation, respectively. Red curves in the FA maps separate the 3 layers in the cerebral wall. Yellow curves in the FA maps separate the cerebral wall from others.

microstructural properties of these layers can be observed from Figure 3. The FA values of the cortical plate were higher than those of the subplate. It was also observed that, in the FA map, the cortical plate becomes darker during prenatal development, indicating loss of anisotropy in the cortical plate. Although a significant decrease in FA values in the cortical plate occurs during the development, there is little change in the thickness of this layer. The situation is opposite for the subplate, which is a key and transient structure in the middle of the cerebral wall during fetal development. The thickness of the subplate increases significantly during the mid-fetal period while this layer remains dark in the FA map and has consistently lower FA values. The FA of the inner layer is higher than that of subplate.

The FA Decreases during Development in a Heterogeneous Manner Across the Cortex

Figure 4 shows the characteristic spatio-temporal FA variation of the cortical plate by mapping this layer for fetal brains of 13, 15, 17, 19, and 21 wg. From 13 to 21 wg, the FA of the overall cortical plate underwent a significant decrease, with the highest value of more than 0.5, dropping to around 0.25 to 0.3 in most cortical areas at 21 wg. This decrease in FA also varied across the cortical plate.

These distinct longitudinal changes of regional FA within the cortical plate were quantitatively measured over time across the 11 cortical ROIs, shown in Figure 5. FA values of all regions decreased during the fetal brain development. There was a general trend from a sharp decrease to a mild decrease from prefrontal and peri-Sylvian areas to other parts of the brain surface. Specifically, most of the prefrontal areas, including the DFC, VFC, and OFC, have a sharper FA decrease than all other areas from 15 to 17 wg. Statistical analysis further demonstrated unique features of the FA time courses of DFC, VFC, OFC, V1C, and IPC whose time courses are significantly different from those of at least 3 different areas (Table 1). In addition, the time courses of FA variation of all other areas except the STC are statistically different from those of at least one another region (Table 1).

Regional Microstructural Changes of the 3 Layers in the Cerebral Wall during Early Fetal and Mid-Fetal Development

The regional microstructural changes of the 3 layers in the cerebral wall that could be delineated by MRI were reflected by comparisons of FA values in the early fetal (13–15 wg) and those in mid-fetal period (17–21 wg), and are shown in

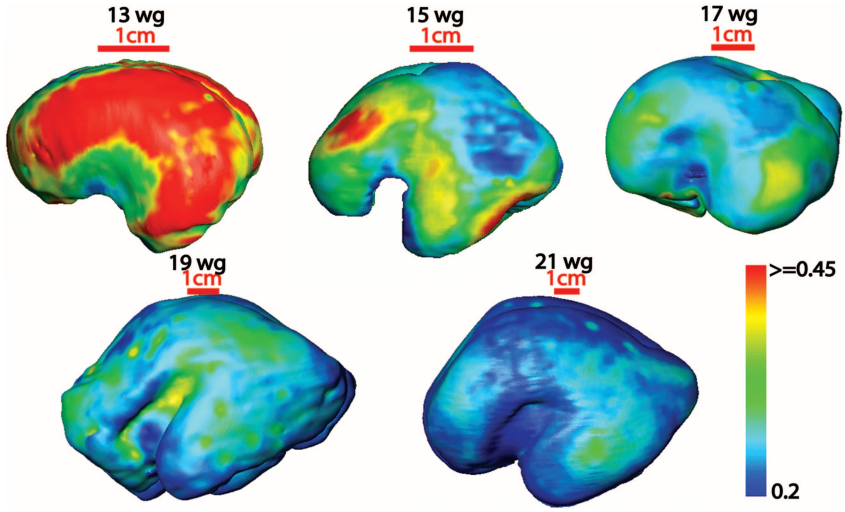

Figure 4. FA mapping of the cortical surface of fetal brains at the gestational ages shown. Color bar indicates the FA values in the cortical surface FA maps.

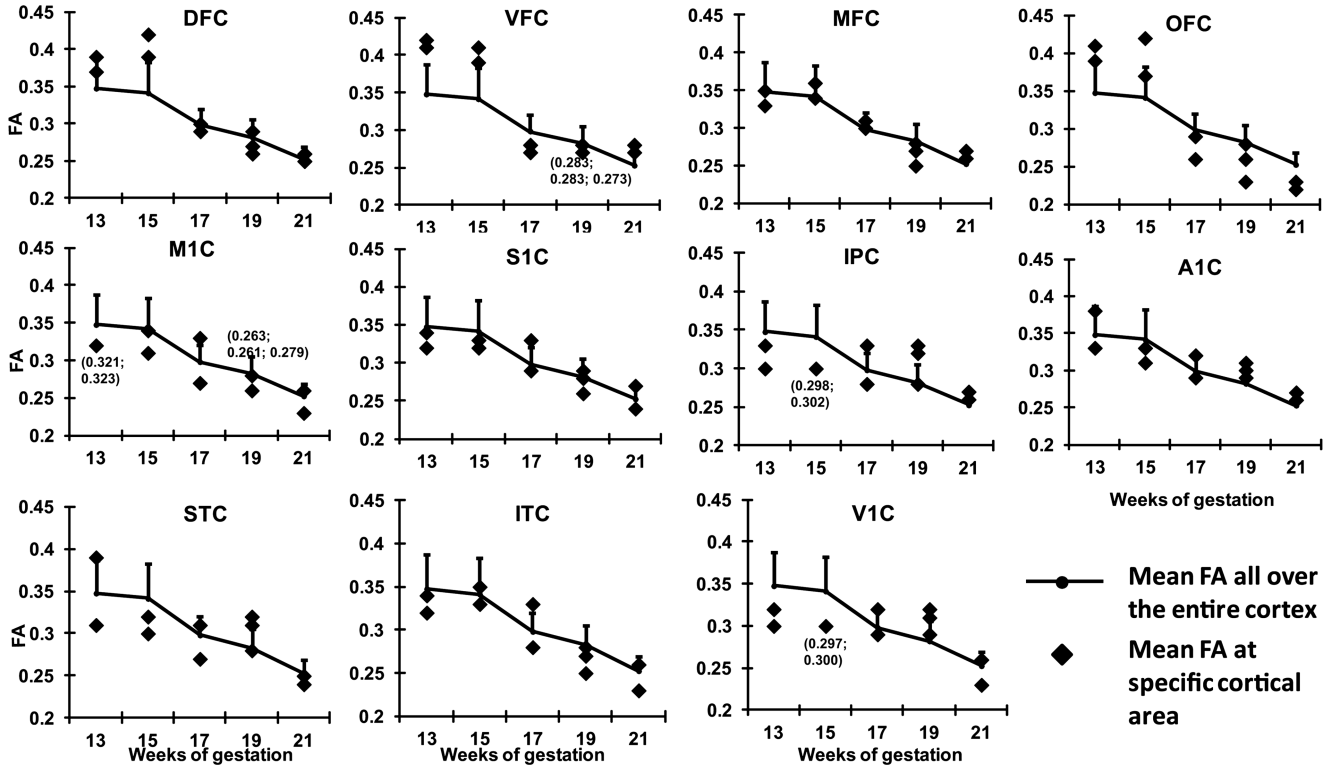

Figure 5. A distinctive time course of FA decreases across 11 ROIs in the cortical plate during the fetal brain development. The FA values averaged across all cortical ROIs are shown as reference curves, with error bars indicating standard deviations. The 2 slightly different measured FA values are marked beside each of the overlapping points.

Table 1

P values from statistical analysis of time courses of FA values among different cortical areas

	DFC	VFC	MFC	OFC	M1C	S1C	IPC	A1C	STC	ITC	V1C
DFC		0.3716	**0.0043**	0.0241	0.1684	0.3707	**0.0041**	0.0841	0.0834	0.1736	**0.0041**
VFC			**0.0041**	0.2085	**0.0043**	**0.0042**	**0.004**	**0.0036**	0.0265	**0.0034**	**0.0035**
MFC				**0.0035**	0.0448	0.372	0.2085	0.497	0.1666	0.3571	0.0452
OFC					0.0847	**0.0036**	**0.0037**	**0.0035**	0.0241	0.0239	**0.0037**
M1C						0.6438	0.0471	0.1685	0.763	0.3799	0.2085
S1C							0.3696	0.5627	0.3771	0.3766	0.0841
IPC								0.2096	0.2508	0.1748	0.7593
A1C									0.2411	0.1697	0.0452
STC										0.4883	0.1736
ITC											0.2085
V1C											

The *P* values smaller than Bonferroni's-correction threshold (0.05/11 = 0.0045) are in bold.

whisker diagrams (Fig. 6). Figure 6 shows that the FA values of the cortical plate were generally the highest and the FA values of the subplate were the lowest across all cortical areas for the stages investigated.

From early fetal to the late mid-fetal period all regions of cortical plate, except the IPC and the V1C, displayed a statistically significant decrease in FA. The FA comparison results in the cortical plate were consistent with the visual observation of the cortical FA map in Figure 4 and regional FA decrease plots across the cortical plate in Figure 5. Also shown in Figure 6, about half of the measured regions displayed significant FA changes in the inner layer from early to mid-fetal developmental period. These changes are coincident with significant changes that also occur in the subplate FA. The changes of FA in the inner layer increase significantly in IPC and V1C and decrease significantly in VFC, M1C, S1C, and ITC.

Quantification of FA Based on Histological Images

With coregistered coronal histological image and the FA map of the 15-wg brain, the ROI (Fig. 7*b*) of 3 layers identified from hematoxylin-stained histological image (Fig. 7*a*) were applied to FA map (Fig. 7*c*). This analysis revealed significant differences of FA values among these layers (Fig. 7*f*). The radial architecture in layer 1 (cortical plate) was clearly visible with the enlarged histological image of the cortical plate (Fig. 7*d*,*e*).

Inner layer consisted of multiple zones. The FA values in this layer reflect integrated effects of the microstructures

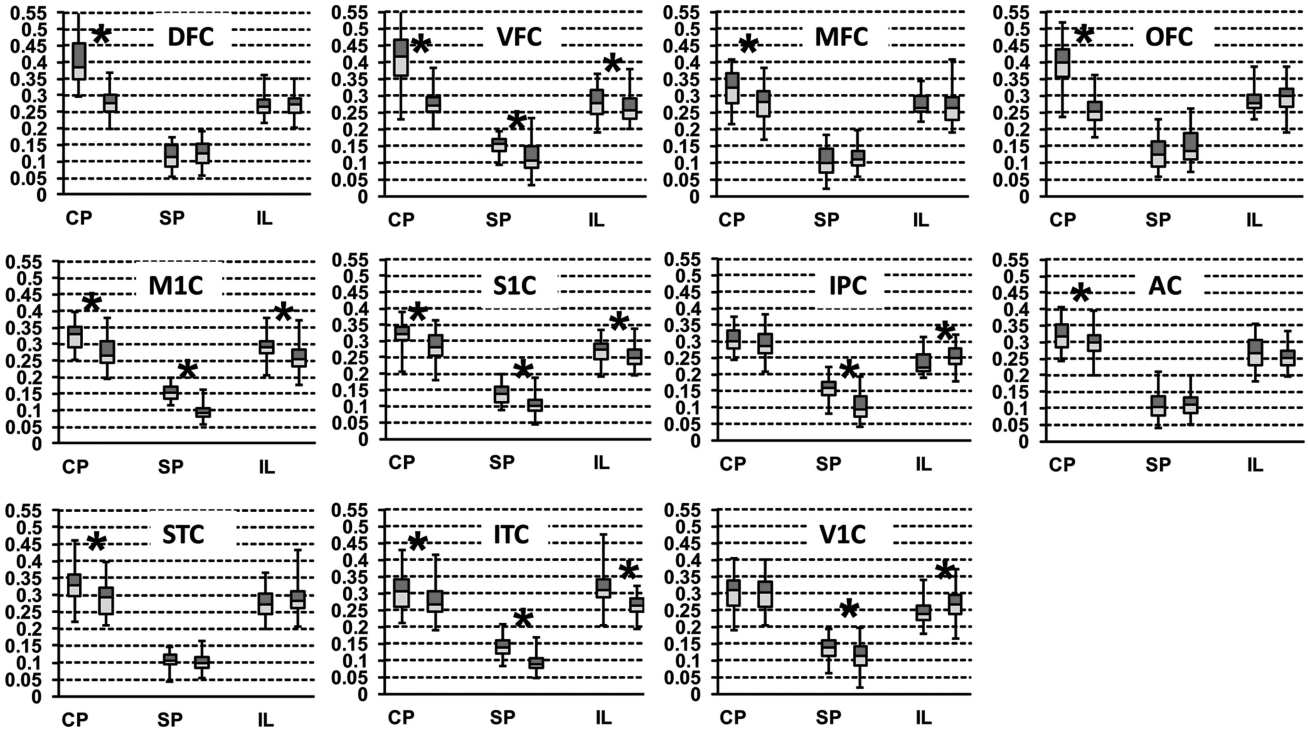

Figure 6. Diagrams of FA measurements of the 11 ROIs from early (left of the box pair) and middle (right of the box pair) fetal period for all 3 layers of the cerebral wall. Abbreviations: CP, cortical plate; SP, subplate; IL, inner layer. Statistically significant differences of FA measurements between early and middle fetal period after FDR correction are marked with asterisks. Blue and red colors indicate the median (50th percentile) to the 75th percentile and the median to the 25th percentile, respectively.

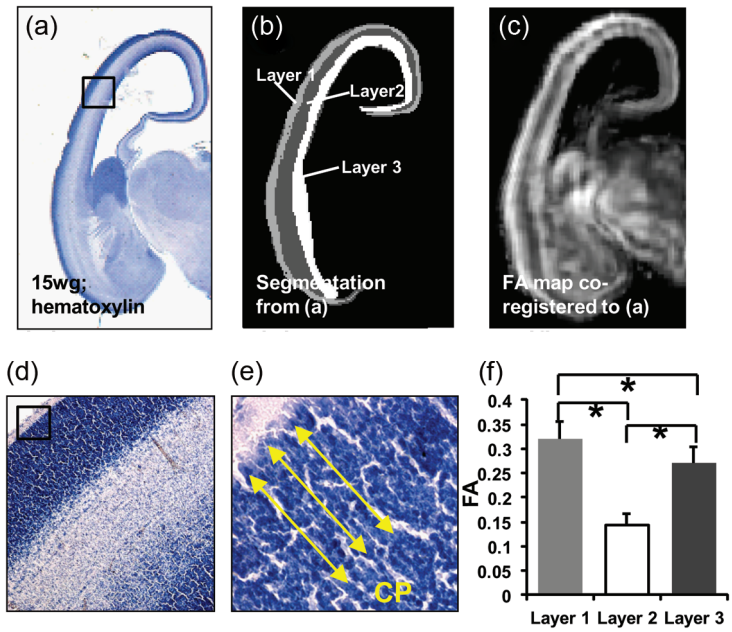

Figure 7. The highly organized layer 1 or cortical plate in hematoxylin-stained histological section is characterized by the highest FA value among all layers in the cerebral wall. (*a*) An image of a hematoxylin-stained histological section of a 15 wg fetal brain. (*d*) A magnified image of the boxed region of (*a*). (*e*) shows a further magnified image of the boxed region in (*d*). Radial microstructures in the cortical plate are clearly visible in (*e*), indicated by yellow lines. (*b*) Segmentation based on contrast of histological image (*a*), dividing the cerebral wall into 3 layers. These layers, layer 1, layer 2 and layer 3, match cortical plate, subplate and inner layer differentiated from the FA map. (*c*) Coregistered FA map after LDDMM transformation. (*f*) FA measurements of these 3 layers. CP in (*e*) is the abbreviation of cortical plate. Asterisks in (*f*) indicate $P < 0.001$.

within these zones. GFAP staining in Figure 8*a* and NF staining in Figure 8*e* revealed both radial (Fig. 8*a*) and tangential (Fig. 8*e*) microstructures, respectively. Microstructures in both directions are indicated by the yellow lines in this layer (Fig. 8*b*, *f*). The radial microstructures are apparent close to the ventricle and are most prominent in the areas that are

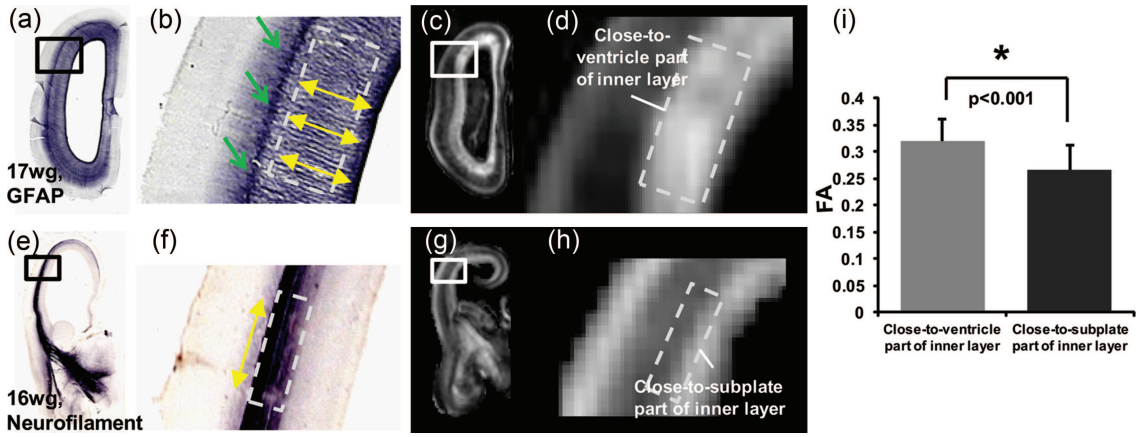

Figure 8. GFAP histological (*a*,*b*) image of a 17 wg fetal brain and the corresponding FA maps (*c*,*d*) are shown in the upper panel. The close-to-ventricle part of the inner layer (layer 3) has clear radial fibers in GFAP images (*a*,*b*). Neurofilament histology image of 16 wg fetal brain and corresponding FA maps (*g*,*h*) are shown in the lower panel. Tangential fibers can be observed in the close-to-subplate part of inner layer (layer 3). The ROIs for FA measurements in (*i*) are shown in (*d*) and (*h*) as dashed boxes, which are consistent with those derived from histology contrasts in (*b*) and (*f*), respectively. The close-to-ventricle part has more uniformly distributed radial fibers and hence has a higher FA value than close-to-subplate region where tangential and radial fibers may cross to each other. Yellow lines in (*b*,*f*) indicate the orientations of the microstructures. Green lines in (*b*) point to the region where GFAP stain color changes and possibly the crossing of tangential and radial fibers takes place. Asterisk in (*i*) indicates $P < 0.001$.

likely to be ventricular, periventricular, and subventricular zones (Fig. 8*b*). The tangential structures in Figure 8*f* delineate the fetal white matter and appear only in part of the inner layer, which is likely to be intermediate zone. Darker GFAP staining at the outer edge of layer 3 is indicated by the green arrows and may correspond to radial glial end-feet. Combined with the observation from Figure 8*f*, showing NF staining of the tangential axonal fibers, it is possible that there are perpendicular crossings of radial and tangential fibers in this part of the layer 3. FA maps of Figure 8*c* and *d* and Figure 8*g* and *h* correspond with the histological images of Figure 8*a* and *b* and Figure 8*e* and *f*, respectively. Owing to the crossing of tangential and radial fibers in the layer 3, the FA values at the ROI (Fig. 8*c*,*d*) with predominantly radial structures are significantly higher (Fig. 8*i*) than those at the ROI (Fig. 8*g*,*h*) with mixed tangential and radial fibers.

Correlation of the Regional Cortical FA Changes with Gene Expression

The cortical FA ratio is a microstructural metric that characterizes the magnitude of cortical plate FA change from early fetal to mid-fetal period. The FA ratio was calculated for each of 11 cortical regions (shown in Fig. 1) and in parallel, the quantifications of 17565 genes from 11 corresponding cortical regions from 9 fetal brain specimens ranging in age from 13 to 21 wg (Kang et al., 2011) were also obtained by gene profiling for each cortical region. The same 11 cortical ROIs were used for gene quantifications and FA ratio calculation (as shown in Fig. 1). For each gene, its expression across the 11 cortical regions was characterized by a vector consisting of 11 quantified numbers. From an analysis of 17565 gene quantifications, 10 genes with the highest correlation with the FA ratio, nominal *P* values, and *P* values after multiple test corrections are listed in Table 2. As a demonstration, Figure 9 shows the vectors of FA ratio and expression of most significantly correlated 5 genes across the 11 cortical regions. The complete cortical FA ratios and expression values of all significantly 10 correlated and anti-correlated genes are tabulated in Supplementary Tables 1 and 2.

Table 2:
List of names, statistics and some related functions of top 10 correlated genes from correlations of FA ratio to all 17565 gene expressions. The correlations between all top 10 genes and FA ratio are statistically significant after FDR correction.

Gene	R	Nominal p (two-sided)	FDR corrected p (two-sided)
SLC17A8	0.962	2.26E-06	0.025
CNTNAP2	0.956	4.19E-06	0.025
ADCY8	0.956	4.25E-06	0.025
POU2F1	0.950	7.54E-06	0.028
DERA	0.949	8.20E-06	0.028
STAG1	0.946	1.11E-05	0.028
DCHS2	0.936	2.24E-05	0.034
C7orf36	0.935	2.44E-05	0.034
ENY2	0.934	2.52E-05	0.034
ITGA9	0.930	3.26E-05	0.038

Discussion

We used DTI as a noninvasive probe to obtain a quantitative spatio-temporal characterization of the entire human fetal cerebral wall. In addition, as complementary investigation approaches, both gene analysis and images of histological sections were incorporated for a comprehensive analysis of the cerebral wall. Specifically, the regional microstructural measures from DTI were linked to the gene expression across the cortex. The distinct patterns of FA time courses across different cortical regions reflect the unique maturation patterns. This analysis revealed both the changes of regional FA values of all cerebral wall layers and microstructural differences within these layers. Genes that have a significant correlation with the regional cortical microstructural changes observed during the fetal brain development were identified in our study.

The immature cortical plate of the cerebral wall is the foundation for the future cerebral cortex and features a columnar organization due to the presence of radial glia (Rakic 1972, 1995; Sidman and Rakic 1973). The immature cortical plate also undergoes maturation into regions that are both cytoarchitectonically (Economo and Koskinas 1925) and functionally unique. The direct mapping of the cortical plate FA in Figure 4 and the time course of regional FA decrease in

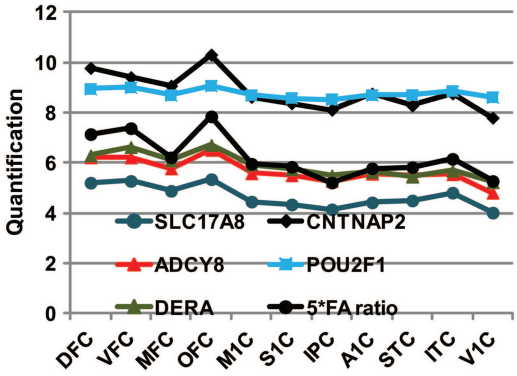

Figure 9. Regional profiles of expression of 5 most significantly correlated genes and anisotropy changes (FA ratio).

Figure 5 reflect a disruption of this initial columnar organization, ongoing differentiation, dendritic growth, and the synapse formation (Mrzljak et al. 1988, 1992) in the immature cortex. A decrease in cortical FA has been reported in the third trimester with DTI data from in vivo scanning of human preterm neonates (26–41 wg in McKinstry et al. 2002; 25–38 wg in deIpolyi et al. 2005) and developmental animal diffusion imaging (Mori et al. 2001; Kroenke et al. 2007; Sizonenko et al. 2007; Huang et al. 2008; Takahashi et al. 2011). DTI of postmortem fetal brains fills a gap in our knowledge of the development of younger human fetal brains and is consistent with the overall trend of cortical FA decrease described in previous developmental human brain studies (McKinstry et al. 2002; deIpolyi et al. 2005). In addition, from an observation of cortical FA map (Fig. 4), quantitative characterization (Fig. 5), and statistical analysis (Table 1), it is clear that the time courses of FA drop in different brain regions are distinct and thus can provide evidence for early cortical patterning and regional differences in cortical maturation. Variable time courses have been characterized with histology (Sidman and Rakic 1982), diffusion MRI (Kroenke et al. 2007; Huang et al. 2008; Kroenke et al. 2009), and conventional T2-weighted MRI (Knutsen et al. 2012) in different regions of the developing human, primate, and rat brains. Our data demonstrate unique FA decreases in the fetal period of human brain development in this study, and suggest that these distinct microstructural changes in different cortical areas may be evolutionarily conserved across different mammalian species.

In the inner layer, which is the layer between the ventricle and subplate, multiple zones can be delineated by histological examination of cresyl violet staining (Kostović et al. 2002) that cannot be distinguished clearly with the contrasts of the FA map given the limitation of resolution. GFAP and NF staining (Fig. 8) revealed that both radial and tangential microstructures in the inner layer could be observed, with pure radial structures close to ventricular boundary and possibly mixed radial and tangential structures close to the subplate. The radial microstructure in Figure 8*a* and *b* further confirmed the presence of the radial glial scaffold (Rakic 1972, 1988, 1995; Sidman and Rakic 1973), which stretches from the ventricular surface and crosses the fetal white matter to reach the subplate. The tangential microstructures in Figure 8*e* and *f*, which are fetal white matter axons, cover the outer region of layer 3 and are immediately surrounded by the subplate. Figure 8 indicates that the FA values in the intermediate zone of layer 3 are the results of the integrated diffusion signals from both radial and tangential microstructures in this layer. The FA values of layer 3 were found to be quite stable across the brain, with the median values around 0.25–0.3 for all 11 ROIs (Fig. 6). The general FA values in this layer are less than those of the cortical plate, but higher than those of the subplate. This pattern resembles the conventional T1-weighted MRI findings in terms of intensities (Kostović et al. 2002). The interference of radial and parallel structures (Fig. 7) may contribute to the lower FA values in layer 3 compared with those of the cortical plate where more uniform radial structures were found. This relative spatio-temporal stability of FA values in layer 3 present across different regions (Fig. 6) is in contrast to the distinction of FA decreases in these same regions of the cortical plate. Despite that there are several regions where significant FA changes can be found during studied periods FA values in the IPC and V1C were significantly higher while those in the VFC, M1C, S1C, and ITC were significantly lower (Fig. 6). Layer 3 is composed mostly of nonmyelinated fibers and includes the highly cellular ventricular and subventricular zones. The FA changes from early fetal to late mid-fetal period in these regions are likely to be affected by multiple factors including the crossing of radial and tangential fibers, axonal growth in the intermediate zone, and dendrite growth in other layers. Axonal growth has the effect of increasing the FA value while crossing of radial and tangential fibers and dendrite growth have the effect of decreasing FA value. The mixed effects from these factors cause an inconsistency in FA changes in these regions.

FA values in the subplate were lowest as the subplate during fetal development contains a high amount of cellular matrix and water (Kostović et al. 2002). They were also consistently low across the brain, around 0.1–0.15 for most regions (Fig. 6). Interestingly, the significant decreases in FA in the subplate in the VFC, M1C, S1C, IPC, ITC, and V1C areas are accompanied by significant changes of FA in layer 3, suggesting cellular and molecular interactions between layers 2 and 3 as cells divide and migrate from layer 3 to the upper layers of the cortex.

Previously, information from gene expression and anatomical structure have been combined to investigate the degree of genetic control over inter-subject variability in the cerebral white matter in the adult human brain (Kochunov, Glahn and Fox et al. 2010), white matter architecture in diseased human brain (Marenco et al. 2007), gray matter structure (Winkler et al. 2010), and the gyrification of the primate brains (Kochunov, Glahn and Lancaster et al. 2010). Generated from 2 different types of tools, the cortical maps of gene profiling and those of the microstructural measurements from DTI were integrated across the identical regions of interest in our study. The integration of the 2 types of datasets in our study enabled us to identify the genes whose heterogeneous expression in different cortical regions may contribute to the heterogeneous FA changes in the same regions. This correlation suggests that unique combinations of different levels of cellular and molecular processes in different cortical and subplate regions underlie the distinctive FA changes measured in these regions. Among the genes with the highest correlation coefficients, several have been implicated in neural development and shown to be associated with neurological and psychiatric disorders (Table 2 and Suppl. Table 1). *CNTNAP2* is a gene important for development of neural circuits. Previous

studies showed the involvement of this gene in etiopathogenesis of autism spectrum disorder, epilepsy, neuronal migration abnormality (Alarcón et al. 2008; Arking et al. 2008; Bakkaloglu et al. 2008; Penagarikano et al. 2011), schizophrenia and bipolar disorder (O'Dushlaine et al. 2011), Tourette syndrome (Verkerk et al. 2003), and intellectual disability (Whitehouse et al. 2011). *ADCY8*, a gene encoding the brain-specific adenylate cyclase, has been previously associated with the bipolar disorder (Zandi et al. 2008; Zhang et al. 2010), while DCHS2, a gene encoding adhesion molecule, was identified as a possible risk factor for Alzheimer's disease (Kamboh et al. 2011).

We speculate that regional differences of FA ratios are the outcome of the biological processes that are modulated by heterogeneous regional gene expression. Our findings suggest that the magnitude of FA changes can potentially serve as a biomarker to evaluate cellular activity levels of synapse formation and cell differentiation during the development of specific brain areas. Our investigation of the relationship of gene and microstructure is exploratory and could potentially benefit from further investigations on the relationship between gene and function and that between microstructure and function. With the advent of ever more sophisticated DTI technology, in utero DTI (e.g. Kasprian et al. 2008) and high-quality DTI data of in vivo preterm neonates (e.g. McKinstry et al. 2002; Maas et al. 2004; deIpolyi et al. 2005) are becoming more available. These advances of DTI technologies suggest the possibility of obtaining sophisticated structural information from *in vivo* fetal brains noninvasively. Establishing a correlation between DTI and gene profiling opens a refreshing window for potentially accessing the cellular activity levels with structural measurements from noninvasive DTI and ultimately assisting clinical prognosis of human brain disorders such as schizophrenia and autism, which are both related to abnormal brain development.

Previous studies on comparing the FA of postmortem brain tissues with that of *in vivo* brain found that formalin fixation alters diffusivity magnitude but not anisotropy (Sun et al. 2003, 2005). This makes it possible to use the DTI data of postmortem fetal brain tissue for FA measurements and analysis of FA time courses. However, the fixation of the studied tissues also made measurement of other DTI-derived metrics, for example, mean diffusivity, less appealing. Therefore, FA was the only metric from DTI used in this study. In this study, each of fixed postmortem fetal brain tissues was scanned with an 11.7-T or a 4.7-T magnet for around 20 h. Previously, Gupta et al. (2005) have reported interesting findings on cortical FA from measurements of unfixed postmortem tissue with 1.5-T magnet and much shorter scan time. The lower magnet strength combined with much shorter scanner time could cause lower SNR for the DTI. In addition, the scans in that study (Gupta et al. 2005) were performed on unfixed brains although the time interval between MRI scan and delivery was reported to be less than 3 h. Human fetal brain tissue is very fragile. Without fixation, the architecture of the fetal brain tissue is quickly disrupted. These factors could cause potential bias of cortical FA measurements and partly explain the differences of their results from those of the present analysis.

The ROIs of FA measurements in this study were restricted by the dissection ROIs used for gene analysis (Johnson et al. 2009; Kang et al. 2011) and correlation between gene and microstructure (FA ratio), although arbitrary ROIs of FA measurements could be chosen given our whole brain FA map. Lack of cortical sulcal landmarks in the studied fetal brains compared with older fetal brains also limited our selection of cortical ROIs for FA measurements. As FA measurements were from postmortem brain tissues, no longitudinal data were available from individual subjects. Hence, temporal FA changes, namely, the FA ratios, include some subject variability. It should also be noted that the correlative results from this study do not prove cause or effect. Instead, with this correlation analysis, we have identified 10 candidate genes whose expression may help explain the variability in rates of microstructural development (FA ratio) for the 11 cortical areas examined.

In conclusion, the spatio-temporal microstructural changes of the cerebral wall during human fetal development were quantitatively characterized with high-resolution DTI data of postmortem brain tissue from 13 to 21 gestational weeks which covers an important period of the fetal brain development. Gene analysis and histology were also integrated to elucidate the relationship between the microstructural changes and gene expression. Distinct time courses of microstructural changes were revealed for 11 anatomically distinguished cortical regions. High FA values correspond to organized radial architecture in histological image. The correlation between DTI measurements and gene analysis suggests that regional variability of the FA ratio may be associated with differential cellular activities of radial glial cell differentiation, neuronal migration, dendritic and axonal growth, synapse formation, and cell adhesion. Establishing the correlation between DTI and gene expression profiling opens a refreshing window for potentially accessing the cellular activity levels with microstructural measurements from noninvasive DTI.

Supplementary Material

Supplementary material can be found at: http://www.cercor.oxfordjournals.org/.

Funding

This work was supported by the National Institute of Health (MH092535, EB009545, AG020012, RR015241, MH089929 and MH081896). L.J.R. is supported by a National Health and Medical Research Council (Australia) principal research fellowship.

Notes

The authors thank Dr Dwight German for discussion about histology data. *Conflict of Interest*: None declared.

References

Alarcón M, Abrahams BS, Stone JL, Duvall JA, Perederiy JV, Bomar JM, Sebat J, Wigler M, Martin CL, Ledbetter DH *et al.* 2008. Linkage, association, and gene-expression analyses identify CNTNAP2 as an autism-susceptibility gene. Am J Hum Genet. 82:150–159.

Allendoerfer KL, Shatz CJ. 1994. The subplate, a transient neocortical structure: its role in the development of connections between thalamus and cortex. Annu Rev Neurosci. 17:185:218.

Arking DE, Cutler DJ, Brune CW, Teslovich TM, West K, Ikeda M, Rea A, Guy M, Lin S, Cook EH *et al.* 2008. A common genetic variant

in the neurexin superfamily member CNTNAP2 increases familial risk of autism. Am J Hum Genet. 82:160–164.
Bakkaloglu B, O'Roak BJ, Louvi A, Gupta AR, Abelson JF, Morgan TM, Chawarska K, Klin A, Ercan-Sencicek AG, Stillman AA *et al*. 2008. Molecular cytogenetic analysis and resequencing of contactin associated protein-like 2 in autism spectrum disorder. Am J Hum Genet. 82:165–173.
Basser PJ, Mattiello J, Le Bihan D. 1994. MR diffusion tensor spectroscopy and imaging. Biophys J. 66:259–267.
Bayer SA, Altman J. 2004. The human brain during the third trimester. Boca Raton, FL: CRC.
Bayer SA, Altman J. 2005. The human brain during the second trimester. Boca Raton, FL: CRC.
Bonferroni CE. 1936. Teoria statistica delle classi e calcolo delle probabilita. In: Pubblicazioni del R Istituto Superiore di Scienze Economiche e Commerciali di Firenze. 8:3–62.
Bystron I, Blakemore C, Rakic P. 2008. Development of the human cerebral cortex: Boulder Committee revisited. Nat Rev Neurosci. 9:110–122.
Caviness VS Jr. 1982. Development of neocortical afferent systems: studies in the reeler mouse. Neurosci Res Prog Bull. 20:560–569.
deIpolyi AR, Mukherjee P, Gill K, Henry RG, Partridge SC, Veeraraghavan S, Jin H, Lu Y, Miller SP, Ferriero DM *et al*. 2005. Comparing microstructural and macrostructural development of the cerebral cortex in premature newborns: diffusion tensor imaging versus cortical gyration. NeuroImage. 27:579–586.
Del Rio JA, Martínez A, Auladell C, Soriano E. 2000. Developmental history of the subplate and developing white matter in the murine neocortex. Neuronal organization and relationship with the main afferent systems at embryonic and perinatal stages. Cereb Cortex. 10:784–801.
Dice LR. 1945. Measures of the amount of ecologic association between species. Ecology. 26:297–302.
Economo CV, Koskinas GN. 1925. Die Cytoarchitektonik der Hirnrinde des Erwachsenen Menschen. Wien und Berlin: Verlagvon Julius Springer.
Gupta RK, Hasan KM, Trivedi R, Pradhan M, Das V, Parikh NA, Narayana PA. 2005. Diffusion tensor imaging of the developing human cerebrum. J Neurosci Res. 81:172–178.
Hawrylycz M, Bernard A, Lau C, Sunkin SM, Chakravarty MM, Lein ES, Jones AR, Ng L. 2010. Areal and laminar differentiation in the mouse neocortex using large scale gene expression data. Methods. 50:113–121.
Honig LS, Herrmann K, Shatz CJ. 1996. Developmental changes revealed by immunohistochemical markers in human cerebral cortex. Cereb Cortex. 6:794–806.
Huang H, Xue R, Zhang J, Ren T, Richards LJ, Yarowsky P, Miller M-I, Mori S. 2009. Anatomical characterization of human fetal brain development with diffusion tensor MRI. J Neurosci. 29: 4263–4273.
Huang H, Yamamoto A, Hossain MA, Younes L, Mori S. 2008. Quantitative cortical mapping of fractional anisotropy in developing rat brains. J Neurosci. 28:1427–1433.
Huang H, Zhang J, Wakana S, Zhang W, Ren T, Richards L-J, Yarowsky P, Donohue P, Graham E, van Zijl P-C *et al*. 2006. White and gray matter development in human fetal, newborn and pediatric brains. Neuroimage. 33:27–38.
Hüppi PS, Maier SE, Peled S, Zientara G, Barnes P, Jolesz FA, Volpe JJ. 1998. Microstructural development of human newborn cerebral white matter assessed in vivo by diffusion tensor magnetic resonance imaging. Pediatr Res. 44:584–590.
Johnson MB, Kawasawa YI, Mason CE, Krsnik Z, Coppola G, Bogdanovic D, Geschwind DH, Mane SM, State MW, Sestan N. 2009. Functional and evolutionary insights into human brain development through global transcriptome analysis. Neuron. 62:494–509.
Kamboh MI, Barmada MM, Demirci FY, Minster RL, Carrasquillo MM, Pankratz VS, Younkin SG, Saykin AJ, The Alzheimer's Disease Neuroimaging Initiative, Sweet RA *et al*. 2011. Genome-wide association analysis of age-at-onset in Alzheimer's disease. Mol Psychiatry. doi:10.1038/mp.2011.135.
Kang HJ, Kawasawa YI, Cheng F, Zhu Y, Xu X, Li M, Sousa AMM, Pletikos M, Meyer KA, Sedmak G *et al*. 2011. Spatio-temporal transcriptome of the human brain. Nature. 478:483–489.
Kasprian G, Brugger PC, Weber M, Krssák M, Krampl E, Herold C, Prayer D. 2008. In utero tractography of fetal white matter development. Neuroimage. 43:213–224.
Kochunov P, Glahn DC, Fox PT, Lancaster JL, Saleem K, Shelledy W, Zilles K, Thompson PM, Coulon O, Mangin JF *et al*. 2010. Genetics of primary cerebral gyrification: heritability of length, depth and area of primary sulci in an extended pedigree of *Papio baboons*. Neuroimage. 53:1126–1134.
Kochunov P, Glahn DC, Lancaster JL, Winkler AM, Smith S, Thompson PM, Almasy L, Duggirala P, Fox PT, Blangero J. 2010. Genetics of microstructure of cerebral white matter using diffusion tensor imaging. Neuroimage. 53:1109–1116.
Kostović I, Judas M, Rados M, Hrabac P. 2002. Laminar organization of the human fetal cerebrum revealed by histochemical markers and magnetic resonance imaging. Cereb Cortex. 12:536–544.
Kostović I, Molliver M. 1974. A new interpretation of the laminar development of cerebral cortex: synaptogenesis in different layers of neopallium in the human fetus. Anat Rec. 178:395 [abstract].
Kostović I, Rakic P. 1980. Cytology and time of origin of interstitial neurons in the white matter in infant and adult human and monkey telencephalon. J Neurocytol. 9:219–242.
Kostović I, Rakic P. 1990. Developmental history of the transient subplate zone in the visual and somatosensory cortex of the macaque monkey and human brain. J Comp Neurol. 297:441–470.
Kostović I, Vasung L. 2009. Insights from in vitro fetal magnetic resonance imaging of cerebral development. Semin Pernatol. 33:220–233.
Kroenke CD, Taber EN, Leigland LA, Knutsen AK, Bayly PV. 2009. Regional patterns of cerebral cortical differentiation determined by diffusion tensor MRI. Cereb Cortex. 19:2916–2929.
Kroenke CD, Van Essen DC, Inder TE, Rees S, Bretthorst GL, Neil JJ. 2007. Microstructural changes of the baboon cerebral cortex during gestational development reflected in magnetic resonance imaging diffusion anisotropy. J Neurosci. 27:12506–12515.
Knutsen AK, Kroenke CD, Chang YV, Taber LA, Bayly PV. 2013. Spatial and temporal variations of cortical growth during gyrogenesis in the developing Ferret brain. Cereb Cortex.. 23:488–498.
Kwan KY, Sestan N, Anton ES. 2012. Transcriptional co-regulation of neuronal migration and laminar identity in the neocortex. Development. 139:35–46.
Levitt P, Barbe MF, Eagleson KL. 1997. Patterning and specification of the cerebral cortex. Annu Rev Neurosci. 20:1–24.
Maas LC, Mukherjee P, Carballido-Gamio J, Veeraraghavan S, Miller SP, Partridge SC, Henry RG, Barkovich AJ, Vigneron DB. 2004. Early laminar organization of the human cerebrum demonstrated with diffusion tensor imaging in extremely premature infants. Neuroimage. 22:1134–1140.
Marenco S, Siuta MA, Kippenhan JS, Grodofsky S, Chang WL, Kohn P, Mervis CB, Morris CA, Weinberger DR, Meyer-Lindenberg A, *et al*. 2007. Genetics contributions to white matter architecture revealed by diffusion tensor imaging in Williams syndrome. Proc Natl Acad Sci USA. 104:15117–15122.
McKinstry RC, Mathur A, Miller JH, Ozcan A, Snyder AZ, Schefft GL, Almli CR, Shimony JS, Shiran SI, Neil JJ. 2002. Radial organization of developing preterm human cerebral cortex revealed by noninvasive water diffusion anisotropy MRI. Cereb Cortex. 12:1237–1243.
Miller MI, Trouve A, Younes L. 2002. On the metrics and euler-lagrange equations of computational anatomy. Annu Rev Biomed Eng. 4:375–405.
Mori S, Itoh R, Zhang J, Kaufmann WE, van Zijl PC, Solaiyappan M, Yarowsky P. 2001. Diffusion tensor imaging of the developing mouse brain. Magn Reson Med. 46:18–23.
Moseley ME, Cohen Y, Kucharczyk J, Mintorovitch J, Asgari HS, Wendland MF, Tsuruda J, Norman D. 1990. Diffusion-weighted MR imaging of anisotropic water diffusion in cat central nervous system. Radiology. 176:439–445.

Mrzljak L, Uylings HB, Kostovic I, Van Eden CG. 1988. Prenatal development of neurons in the human prefrontal cortex: I. A qualitative Golgi study. J Comp Neurol. 271:355–386.
Mrzljak L, Uylings HB, Kostovic I, van Eden CG. 1992. Prenatal development of neurons in the human prefrontal cortex. II. A quantitative Golgi study. J Comp Neurol. 316:485–496.
Mukherjee P, Miller JH, Shimony JS, Philip JV, Nehra D, Snyder AZ, Conturo T-E, Neil JJ, McKinstry RC. 2002. Diffusion-tensor MR imaging of gray and white matter development during normal human brain maturation. Am J Neuroradiol. 23:1445–1456.
Neil JJ, Miller J, Mukherjee P, Hüppi PS. 2002. Diffusion tensor imaging of normal and injured developing human brain-a technical review. NMR Biomed. 15:543–552.
Neil JJ, Shiran SI, McKinstry R, Schefft G, Snyder A, Almli CR, Akbudak E, Aronovitz JA, Miller JP, Lee BC, Conturo TE. 1998. Normal brain in human newborns: apparent diffusion coefficient and diffusion anisotropy measured by using diffusion tensor MR imaging. Radiology. 209:57–66.
O'Dushiaine C, Kenny E, Heron E, Donohoe G, Gill M, Morris D. International Schizophrenia Consortium, Corvin A. 2011. Molecular pathways involved in neuronal cell adhesion and membrane scaffolding contribute to schizophrenia and bipolar disorder susceptibility. Mol Psychiatry. 16:286–292.
O'Rahilly R, Műller F. 2006. Embryonic human brain: an atlas of developmental stages. Hoboken, NJ: John Wiley & Sons, Inc.
Partridge SC, Mukherjee P, Henry RG, Miller SP, Berman JI, Jin H, Lu Y, Glenn OA, Ferriero DM, Barkovich AJ, Vigneron DB. 2004. Diffusion tensor imaging: serial quantitation of white matter tract maturity in premature newborns. Neuroimage. 22:1302–1314.
Penagarikano O, Abrahams BS, Herman EI, Winden KD, Gdalyahu A, Dong H, Sonnenblick LI, Gruver R, Almajano J, Bragin A *et al*. 2011. Absence of CNTNAP2 leads to epilepsy, neuronal migration abnormalities, and core autism-related deficits. Cell. 147:235–246.
Rakic P. 1972. Mode of cell migration to the superficial layers of fetal monkey neocortex. J Comp Neurol. 145:61–83.
Rakic P. 1995. A small step for the cell – a giant leap for mankind: a hypothesis of neocortical expansion during evolution. Trends Neurosci. 18:383–388.
Rakic P. 1988. Specification of cerebral cortical areas. Science. 241:170–176.
Rakic P, Suner I, Williams RW. 1991. A novel cytoarchitectonic area induced experimentally within the primate visual cortex. Proc Natl Acad Sci USA. 88:2083–2087.
Sidman RL, Rakic P. 1982. Development of the human central nervous system. In: Haymaker W, Adams RD, editors. Histology and histopathology of the nervous system. Springfield, IL: Thomas. p. 3–145.
Sidman RL, Rakic P. 1973. Neuronal migration, with specific reference to developing human brain: a review. Brain Res. 62:1–35.
Shaffer JP. 1995. Multiple hypothesis testing. Annu Rev Pscychol. 46:561–584.
Sizonenko SV, Camm EJ, Garbow JR, Maier SE, Inder TE, Williams CE, Neil JJ, Hüppi PS. 2007. Developmental changes and injury induced disruption of the radial organization of the cortex in the immature rat brain revealed by in vivo diffusion tensor MRI. Cereb Cortex. 17:2609–2617.
Sun SW, Neil JJ, Liang HF, He YY, Schmidt RE, Hsu CY, Song SK. 2005. Formalin fixation alters water diffusion coefficient magnitude but not anisotropy in infracted brain. Magn Reson Med. 53:1447–1451.
Sun SW, Neil JJ, Song SK. 2003. Relative indicies of water diffusion anisotropy are equivalent to live and formalin-fixed mouse brains. Magn Reson Med. 50:743–748.
Takahashi E, Dai GP, Rosen GD, Wang RP, Ohki K, Folkerth RD, Galaburda AM, Wedeen VJ, Grant PE. 2011. Developing neocortex organization and connectivity in cats revealed by direct correlation of diffusion tractography and histology. Cereb Cortex. 21:200–211.
Takahashi E, Folkerth RD, Galaburda AM, Grant PE. 2012. Emerging cerebral connectivity in the human fetal brain: An MR tractography study. Cereb Cortex. 22:455–464.
Thornton JS, Ordidge RJ, Penrice J, Cady EB, Amess PN, Punwani S, Clemence M, Wyatt JS. 1997. Anisotropic water diffusion in white and gray matter on the neonatal piglet brain before and after transient hypoxia ischemia. Magn Res Imaging. 15:433–440.
Toga AW, Thompson PM, Sowell ER. 2006. Mapping brain maturation. Trends Neurosci. 29:148–159.
Vasung L, Huang H, Jovanov-Milošević N, Pletikos M, Mori S, Kostović I. 2010. Development of axonal pathways in the human fetal fronto-limbic brain: histochemical characterization and diffusion tensor imaging. J Anat. 217:400–417.
Verkerk AJ, Mathews CA, Joosse M, Eussen BH, Heutink P, Oostra BA, Tourette syndrome Association International Consortium for Genetics. 2003. CNTAP2 is disrupted in a family with Gilles de la Tourette syndrome and obsessive compulsive disorder. Genomics. 82:1–9.
Whitehouse AJ, Bishop DV, Ang QW, Pennell CE, Fisher SE. 2011. CNTNAP2 variants affect early language development in the general population. Genes Brain Behav. 10:451–456.
Winkler AM, Kochunov P, Blangero J, Almasy L, Zilles K, Fox PT, Duggirala R, Glahn DC. 2010. Cortical thickness or grey matter volume? The importance of selecting the phenotype for imaging genetics studies. Neuroimage. 53:1135–1146.
Zandi PP, Zollner S, Avramopoulos D, Willour VL, Chen Y, Qin ZS, Burmeister M, Miao K, Gopalakrishnan S, McEachin R, Potash JB, Depaulo JR Jr, Mclnnis MG. 2008. Family-based SNP association study on 8q24 in bipolar disorder. Am J Med Genet B. 147B:612–618.
Zhang J, Chen Y-B, Hardwick J-M, Miller M-I, Plachez C, Richards LJ, Yarowsky P, van Zijl P, Mori S. 2005. Magnetic resonance diffusion tensor microimaging reveals a role for Bcl-x in brain development and homeostasis. J Neurosci. 25:1881–1888.
Zhang J, Richards L-J, Yarowsky P, Huang H, van Zijl P-C, Mori S. 2003. Three dimensional anatomical characterization of the developing mouse brain by diffusion tensor microimaging. Neuroimage. 20:1639–1648.
Zhang P, Xiang N, Chen Y, Sliwerska E, Mclnnis MG, Burmeister M, Zollner S. 2010. Family-based association analysis to finemap bipolar linkage peak on chromosome 8q24 using 2,500 genotyped SNPs and 15,000 imputed SNPs. Bipolar Disord. 12:786–792.